The following supplements accompany the article

Bordeaux wine quality and climate fluctuations during the last century: changing temperatures and changing industry?

Pablo Almaraz*

*Corresponding author: palmaraz@gmail.com

Climate Research 64: 187–199 (2015)

SUPPLEMENT 1. ADDITIONAL INFORMATION

S1. Reliability of temperature data from the Mérignac/Bordeaux Airport weather station

Weather stations located within highly urbanized areas may be affected by the so-called Urban Heat Island effect (UHI, Arnfield 2003, Kalnay & Cai 2003). That is, a metropolitan area is usually significantly warmer than the surrounding rural areas because of human activities. Although the global temperature bias introduced by the UHI effect is of just 0.05 ^{o}C (IPCC 2013), some individual weather stations may suffer from this effect more severely. Given that the Mérignac/Bordeaux Airport weather station used in the present study is located within the Bordeaux city area, the UHI may be significantly biasing the growing season temperatures estimated in the present study. To assess the reliability of this station as representative of the weather for the whole Bordeaux area, three sets of alternative temperature time series were explored (See Fig. S1):

1) Following Jones et al. (2005), data from a 0.5^{o} x 0.5^{o} gridded monthly temperature time series centered in the Mérignac/Bordeaux Airport weather station were downloaded from the Global Historical Climatological Network (GHCN v3). It should be noted, however, that at this level of spatial resolution the only publicly available station data is precisely that from the Mérignac/Bordeaux Airport weather station (MÉRIGNAC GHCN v3, ID: 61507510000; See also the gridded Monthly station data in the KNMI webpage). In contrast to the GHCN v2 used by Jones et al. (2005), the version 3 is highly suitable because it was homogenized using the pairwise correlation method of Menne & Williams (2009). This method effectively removes undocumented shifts in time series by pair-wise correlating the focal series with a network of observing stations. These shifts are induced mainly by local land-use changes and the UHI effect. The available homogenized time series starts in 1951. Fig. S2 shows the time series of growing season temperatures from the uncorrected (non-homogenized) Mérignac/Bordeaux Airport weather station (daily data downloaded from the KNMI) and the available growing season temperature data from the same station downloaded from the GHCN v3 webpage. Both series are highly correlated (r = 0.973, $P_{\mathrm{boot}} < 0.001$), and the average bias in growing season temperatures of the non-homogenized data relative to the homogenized series is small (0.17 ± 0.33 ^{o}C). Moreover, conducting the analysis with either of both series produce virtually the same results, although the optimum average growing season temperature is upward biased by a 6% when the non-homogenized KNMI series is used. Therefore, it is safe to merge both time series (KNMI, 1920-1950; GHCN v3, 1951-2009); this dataset will be named hereafter "merged dataset".

2) The merged dataset was compared to the time series of growing season temperatures from Chevet et al. (2011), which span the same period of the present study. The weather station used by Chevet et al. (2011) is located within the Pauillac Apéllation, 40 Kms. to the North West of the Mérignac weather station. Both time series are highly correlated (r = 0.90, P_{boot} < 0.001). Interestingly however, although this weather station should not be significantly affected by the UHI effect, its average growing season temperature is slightly larger (17.40 ± 0.93 °C) than the average temperature of the homogenized Mérignac station data (17.17 ± 0.89 °C), and even larger than the non-homogenized data (17.27 ± 1.04 °C). In any case, both time series show the same cyclic structure across time (Fig. S3b-d), and only during the first half of the 1980s was there a short, transient loss in the covariation among both (Fig. S3d).

3) The merged dataset was also compared to the temperature data used by Lecocq & Visser (2006). These authors regressed Bordeaux wine prices on temperature data from ten local weather stations spread within the Bordeaux wine area (See Fig. S1). These data consist on June-July and August-September average temperatures for the period 1993-2002. The data from these stations, along with the data from the merged dataset, is shown in Fig. S4. Interestingly, the average temperature of the merged dataset for this period is virtually identical to the temperature averaged across the ten weather stations (excluding that of Mérignac). Moreover, many of the weather stations studied by Lecocq & Visser (2006) show consistently larger temperature than the merged dataset, even though these stations should not be significantly affected by the UHI effect.

Overall, these analyses suggest that the merged temperature dataset from the Mérignac/Bordeaux Airport weather station used in the present study is highly reliable as representative of the temperature within the whole Bordeaux wine area. Indeed, although Lecocq & Visser (2006) found slight spatial variations in climate within this area, these authors show that using the temperature data from the Mérignac/Bordeaux Airport weather station instead of the data from the local weather stations produce essentially the same results.

S2. Fitting of the TVCs model accounting for within-season temperature variability

Statistical regression theory predicts that sampling error, or any type of uncertainty in a predictor variable, will cause an *attenuation* of the regression coefficient for that variable (Carroll et al. 2006). To account for this effect, and to assess the sensitivity of the results of the present study to the uncertainty in the estimation of growing season temperatures, an alternative TVCs model will be fitted that incorporates an observation model analogous to the model for wine rating uncertainty. This model has the form:

$$T_{obs,t} \,|\, T_t \sim N(T_t, \mu_t^2)$$

were $T_{obs,\,t}$ is the observed growing season temperature for year t, and T_t is the latent growing season temperature for year t. An estimate for the time-varying uncertainty in growing season temperature at year t is encapsulated in $\mu^2{}_t$. In the absence of other information, the best estimate for this uncertainty is simply the within-season variance in temperature during the growing season. For example, a year with a high average temperature and a low within-season variance will have a stronger relative impact on model estimation than a year of similar temperature but with higher within-season variance. The net effect will be a reduction in the variance of the estimated effect of temperature on wine quality in the former case, and an increase in estimation variance in the later. Therefore, the fitted model will be fully stochastic (West & Harrison 1997), since both the predictor and the response variable are measured with uncertainty.

The results of this alternative fitting are shown in Fig. S5. The profile of the time-varying effect of temperature on wine quality is virtually the same, but the proportion of variance in wine quality explained by temperature increased when the within-season variance is taken into account. This is due to the attenuation effect mentioned above. Indeed, the fitting of this model was even better than the model ignoring within-season variance in temperature estimation (WAIC: 166.635 ± 10.703; see Table 1 in the accompanying paper). It is also interesting to note that the uncertainty in the estimation of the optimum growing season temperature is now also larger: this is expected, since the within-season variance propagates to the estimated optimum during simulation. Overall, these results reinforce the findings of the accompanying paper that ignores within-season variance, since they suggest that uncertainty in the estimation of growing season temperatures does not qualitatively modify the results.

S3. Estimating uncertainty in wine quality ratings from independent raters

Table S1 shows the database used in the present study. Table S3 shows the Spearman's rank-order correlations among 10 series of Bordeaux wine quality ratings obtained from the literature, plus the correlation among these time series and the variables Year and Growing season temperature. As shown, the correlation among the wine quality ratings is very large, even though some of them refer to different apéllations within the Bordeaux wine area. While 8 out of 10 display temporal trends, only 6 out of 10 show a significant correlation with temperature.

To obtain an empirical approximation for wine quality rating uncertainty, three of the gathered time series were selected: Robert Parker (http://www.erobertparker.com; data averaged for the whole Bordeaux region); Jeff Leve (http://www.thewinecellarinsider.com) and Tom Stevenson (2001; data averaged for the whole Bordeaux region). These are highly reputed and critically exposed wine experts, so the effects of their evaluations on wine prices and customer choices should be large (Robert & Reagans 2007). After re-scaling these ratings to a 0-20 scale, to make them comparable to the Tastet & Lawton rating system, a large concordance was found among the four raters (Intraclass correlation coefficient: 0.93; 95% Confidence Interval: 0.87-0.96). The value of τ_t^2 obtained from the yearly inter-rater variability averaged from 1970 to 2000 was relatively low, but somewhat larger than previous estimations for recent vintages (Cardebat & Figuet 2013). Indeed, a negative exponential relationship was found between the coefficients of variation of yearly inter-rater judgments and the averaged vintage quality of the rescaled ratings (Fig. 1b in the accompanying paper). This means that inter-rating uncertainty decreases with wine quality for the datasets studied. Therefore, a negative exponential function was implemented in the observation model (eqn. 1.5) to predict the value of rating variance, τ_t^2, from the observed vintage rating.

S4. Parameter estimation method and model comparison

Through Markov Chain Monte Carlo, posterior distributions for parameter and latent wine quality ratings are derived from the product of the likelihood and prior distributions of parameters through stochastic simulation (Gelman et al. 2013a). In environmental sciences the most common strategy is to use the Gibbs sampler to sample from the posterior distribution (e.g., Clark 2007). However, this algorithm uses a random walk to propose future states for the iterative Markov chain (Gelman et al. 2013a), which makes the convergence to a stationary posterior distribution highly inefficient. The relatively complex structure of the TVCs model may induce large cross-correlations among parameters during simulation from the posterior distribution, with further increases in sampling inefficiency. Therefore, a Hamiltonian/Hybrid Monte Carlo approach (HMC; Neal 2011) will be followed here. HMC was originally proposed for simulation in quantum chromodynamics (Duane et al. 1987) and provides the advantage of merging MCMC simulation with molecular dynamics, so that the future states in the Markov Chain are now proposed by physical system (Hamiltonian) dynamics and not by a random process. In brief, Hamiltonian dynamics regards the motion of an object as the sum of its potential and kinetic energies, with the assumption that the total energy (the Hamiltonian) is conserved. This perspective is exploited to implement a Hamiltonian scheme as a proposal function for the joint posterior distribution, so that sampling is performed through simulation of the location and momentum of states in the Markov Chain constrained to the Hamiltonian condition (see Neal 2011 for technical details).

Priors were set to improper uniform distributions defined in the entire real line for the location parameters, I, $\alpha_{\cdot}$, $\beta_{\cdot}$, $l_{\cdot}$ ~ U(-∞, +∞), and uniform distributions with a lower truncation at 0 for the standard deviations of the scale (variance) parameters: σ_t, $\rho_{\cdot}$ ~ U(0, +∞). Given that the quadratic coefficients of the TVCs model were sometimes very close to 0 (see Results) the estimated time-varying optimum temperature was truncated between 10 and 35 ^{0}C during posterior simulations. Three Markov chains with diffuse random initial values were run during 4000 iterations for both models, and statistical summaries of parameters and latent vintage ratings were constructed from the posterior distributions after discarding the first 3000 iterations as a warmup; 68% posterior credible intervals, equivalent to 1 standard deviation, were constructed for the time-varying coefficients.

The Watanabe/Akaike, or Widely Applicable, Information Criterion, WAIC, was calculated as (Gelman et al. 2013b):

$$WAIC = -2\left(\sum_{i=1}^{n}\log\left(\frac{1}{S}\sum_{s=1}^{S}p\left(y_i \mid \theta^s\right)\right)-\sum_{i=1}^{n}V_{s=1}^{S}\left(\log p\left(y_i \mid \theta^s\right)\right)\right) \quad \text{S1.1}$$

The first summation in the right-hand side of Eqn. S2.1 is the *log* pointwise predictive density of the posterior simulations, $p(y_i|\theta^s)$, drawn from S Monte Carlo iterations and summed across the n observations (90 years in this case). The second summation is the effective number of parameters, calculated as the sum of the posterior sample variances of the *log* predictive densities for each data point. It can be seen that the WAIC is asymptotically equivalent to leave-one-out cross-validation (Gelman et al. 2013b) but, in contrast to alternative model selection tools, it is fully Bayesian because it is not based on point estimation, as all the observations are used to compute the log predictive density and its variance. This increases the stability of the WAIC (Gelman et al. 2013b). The original WAIC is multiplied by -2 to use the deviance scale of the DIC and AIC, and thus allow similar inference: a model minimizing the WAIC in Eqn. S2.1 is better at out-of-sample predictive fit; that is, if a model should be used to predict unobserved values, that minimizing the WAIC should be selected.

Table S1 Raw data used to conduct the analyses of the accompanying paper

		Wine Quality Expert Ratings			
Year	**Growing season temperature (^oC)**	**Tastet & Lawton**	**Jeff Leve**	**Robert Parker**	**Tom Stevenson**
1920	16.51	16			
1921	17.42	18			
1922	16.69	15			
1923	16.67	15			
1924	16.55	17			
1925	16.49	13			
1926	16.94	18			
1927	16.42	13			
1928	17.16	19			
1929	16.86	20			
1930	16.29	11			
1931	15.74	4			
1932	16.27	10			
1933	17.57	11			
1934	17.63	17			
1935	16.82	9			
1936	15.84	5			
1937	16.93	17			
1938	15.88	12			
1939	15.91	12			
1940	16.79	13			
1941	16.09	2			
1942	17.54	11			
1943	18.36	17			
1944	17.87	10			
1945	18.61	19			
1946	16.41	10			
1947	18.58	18			
1948	16.64	15			
1949	18.34	18			
1950	17.38	16			
1951	16.32	8			
1952	17.37	17			
1953	16.98	18			
1954	15.63	9			
1955	17.40	18			
1956	15.92	9			
1957	16.38	12			
1958	16.67	12			
1959	17.73	19	95		
1960	16.67	12	60		
1961	17.52	20	96		
1962	16.50	17	87		
1963	15.92	3	60		

1964	17.47	17	83		
1965	15.57	3	50		
1966	16.70	17	86		
1967	16.42	14	80		67.5
1968	16.42	6	60		25
1969	16.75	12	60		61
1970	16.87	18	87	86.8	88.5
1971	17.42	17	85	84.2	83
1972	15.52	10	65		40
1973	17.65	12	65		79
1974	16.65	12	65		60
1975	17.48	17	84	87	90
1976	18.08	16	80	79.2	80
1977	15.92	11	70		45
1978	16.40	17	85	86	85
1979	16.72	16	84	86	85
1980	16.58	13	70	77.2	76.5
1981	17.22	16	84	83.8	82
1982	17.65	19	96	92.4	98
1983	17.87	17	87	89.8	86.5
1984	16.71	12	80		70
1985	17.05	18	90	88.2	92
1986	16.53	18	88	89.6	87.5
1987	17.68	14	82	80.2	76.5
1988	17.65	17	89	87.6	88
1989	18.62	19	95	89.8	95
1990	18.78	19	96	94.4	91
1991	18.08	13	65	68	76.5
1992	18.00	12	70	77.2	78
1993	16.96	14	85	82.4	83.5
1994	17.64	15	87	86.6	85
1995	17.84	17	90	89.8	90
1996	17.23	18	89	88.4	92.5
1997	18.54	15	85	85	81.5
1998	17.73	17	92	91.8	87.5
1999	18.51	16	86	88.2	86.5
2000	18.16	19	100	95.6	90
2001	17.77	17	92	89	
2002	17.30	16	89	87	
2003	19.83	18	93	89	
2004	18.12	17	91	87.8	
2005	18.68	20	100	96.6	
2006	19.12	17	91	88	
2007	17.85	16	87	86.2	
2008	17.30	17	91	92	
2009	18.43	19	97	97	

Table S2. Descriptive statistics for all the time series used in the present study. Note that the wine quality rating time series from Robert Parker and Tom Stevenson are averages for the whole Bordeaux area (see Table S3).

Time series	N	Mean	Min	Max	SD
Growing season temperature (GST), ^{o}C	90	17.17	15.52	19.83	0.89
Number of days with GST > 30 ^{o}C	81	16.95	0	54	9.67
GST of days with GST > 30 ^{o}C	80	32.31	30.71	34.20	0.67
Tastet & Lawton's Wine Quality Rating	90	14.50	2	20	4.19
Jeff Leve's Wine Quality Rating	51	82.82	50	100	12.17
Robert Parker's Wine Quality Rating	35	87.08	68	97	5.81
Tom Stevenson's Wine Quality Rating	34	78.91	25	98	16.12

Table S3. Spearman's rank-order correlations among the 10 time series of Bordeaux wine quality ratings gathered from the literature, plus the variables Year and Growing season temperature. Values in bold type denote significant correlations ($P_{boot} < 0.05$).

	#	Time series	1	2	3	4	5	6	7	8	9	10	11
	1	Year											
	2	Growing season temperature	**0.49**										
	3	Tastet & Lawton	**0.26**	**0.62**									
	4	Jeff Leve	**0.51**	**0.61**	**0.91**								
	5	Jones & Davis (2000)	0.14	**0.68**	**0.90**	**0.85**							
Robert Parker	**6**	St. Jullian / Pauillac / St. Estéphe	**0.37**	0.25	**0.87**	**0.83**	**0.87**						
Robert Parker	**7**	Margaux	**0.53**	0.26	**0.66**	**0.74**	**0.55**	**0.75**					
Robert Parker	**8**	Graves	**0.32**	0.18	**0.72**	**0.78**	**0.76**	**0.73**	**0.72**				
Robert Parker	**9**	Pomerol	0.30	0.29	**0.66**	**0.75**	**0.76**	**0.63**	**0.54**	**0.80**			
Robert Parker	**10**	St. Émilion	**0.55**	**0.45**	**0.76**	**0.92**	**0.81**	**0.80**	**0.81**	**0.82**	**0.79**		
Tom Stevenson	**11**	Médoc & Graves	**0.43**	**0.40**	**0.94**	**0.89**	**0.84**	**0.91**	**0.68**	**0.70**	**0.65**	**0.71**	
Tom Stevenson	**12**	St. Émilion & Pomerol	**0.53**	**0.55**	**0.91**	**0.92**	**0.85**	**0.85**	**0.59**	**0.77**	**0.84**	**0.82**	**0.93**

Figure S1: Location of Bordeaux wine area, in Southwestern France, and the 37 Wine Apéllations within the region. Arrows and boxes denote the location of the weather stations studied by Lecocq & Visser (2006) and used in the present study for validating the merged Mérignac/Bordeaux airport station data. Map by Domenico-de-ga, Creative Commons Attribution-Share Alike 3.0.

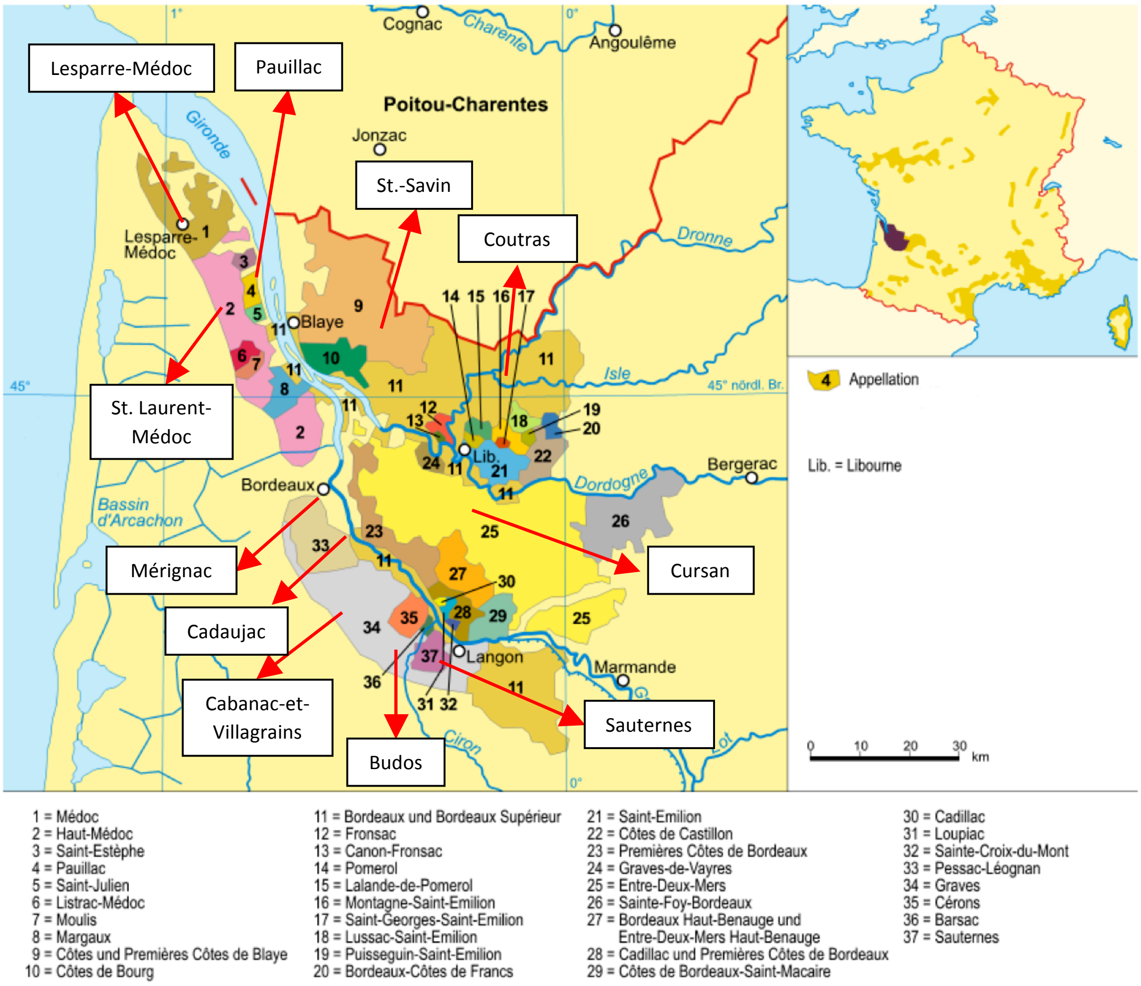

Figure S2: Comparison of the non-homogenized time series of April-October temperatures from the Mérignac/Bordeaux Airport weather station obtained from the KNMI (1920-2009, in blue), the homogenized temperature time series of the same station extracted from the GHCN, version 3 (1951-2009, in red), and the times series data used by Jones et al. (2005), based on an earlier version of the GHCN (in green). This data correspond to an averaged 0.5° x 0.5° gridded monthly temperature dataset from the GHCN v2 centered in the Mérignac/Bordeaux Airport weather station (Jones et al. 2005), and were homogenized using the method by Easterling & Peterson (1995). Even after the Menne & Williams (2009) correction for homogeneization of the GHCN v3, the correlation between both time series is very large (r = 0.95, $P < 0.001$). Using either dataset yields to the same results.

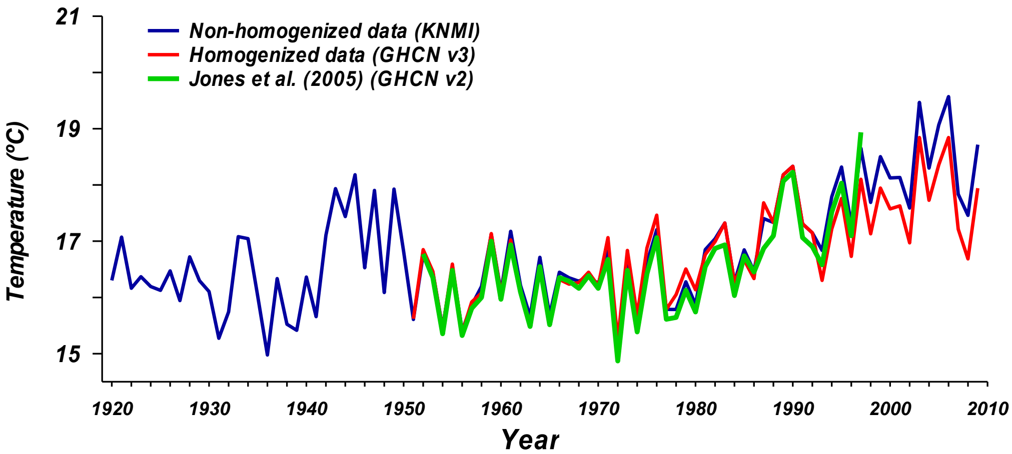

Figure S3: Comparison of growing season temperature data from Pauillac (Chevet et al. 2011) to the merged temperature data from the Mérignac/Bordeaux Airport weather station used in the present study (homogenized from 1951-2009). In b) the Continuous Morlet Wavelet Transform (Grinsted et al. 2004) is shown for each time series; these figures extend the time series into the frequency domain, thus depicting the time-evolution of the power of each periodic constituent (shown in the scale on the right); c) The Cross Wavelet transform, which identify regions in the time-frequency space where the time series show high common power; d) The Wavelet Coherence plot identify regions in the time-frequency space where the two time series co-vary, but does not necessarily have high power. In all plots, the power of the time-frequency regions surrounded by thick lines is statistically significant after 10,000 bootstrap simulations (reddened colors). The direction of the arrows in c) and d) indicate the phase of the co-variation (in-phase when the arrow points to the right). Values within the cone of influence (shaded in grey) are not statistically reliable.

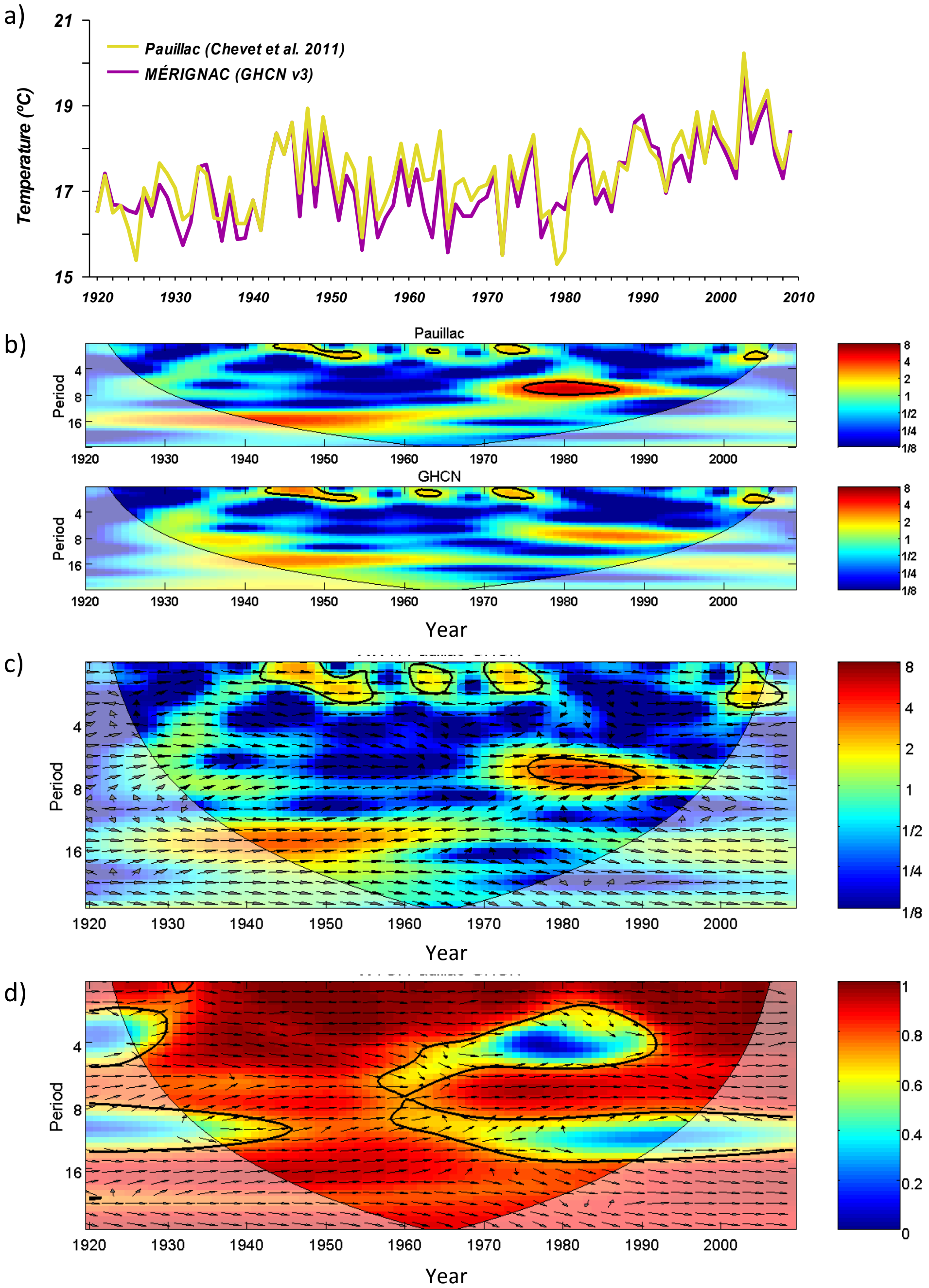

Figure S4: Average temperature (± 1 SD) during June-July (JJ) and August-September (AS) measured in the 10 weather stations within the Bordeaux wine area studied by Lecocq & Visser (2006) from 1993 to 2002 (See map in Fig. S1). The label "Global" depicts the meta-analytic average and standard deviation of the 10 weather stations. The label "MÉRIGNAC GHCN v3" depicts the average temperature of the homogenized data from the Mérignac/Bordeaux Airport weather station used in the present study.

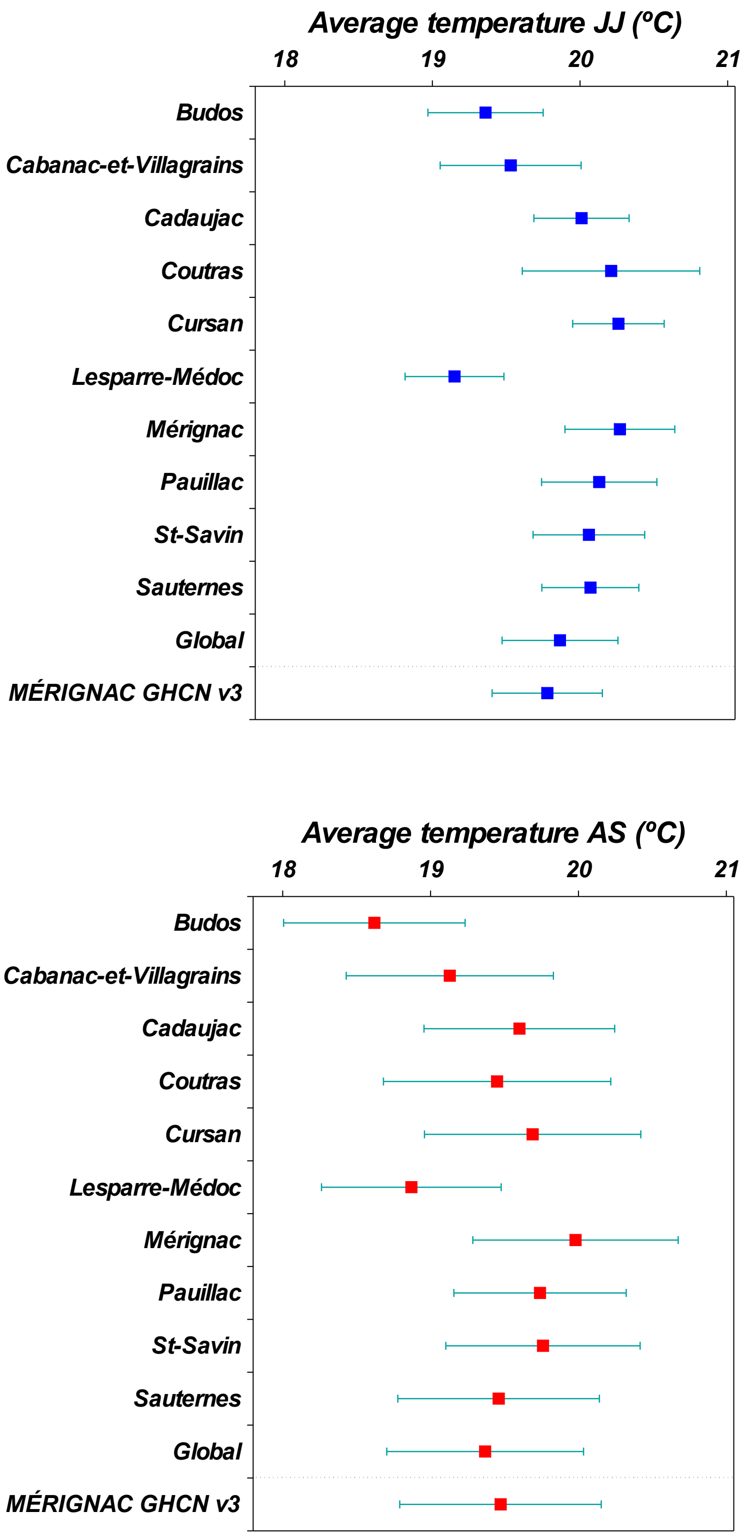

Figure S5: Results of the fitting of the TVCs model to the time series of Bordeaux wine quality ratings accounting for uncertainty in the estimation of growing season temperatures. The temperature values are shown in a), along with the 95% confidence interval arising from the within-season temperature variability. The linear time-varying effect of temperature on wine quality is shown in b), the quadratic time-varying effect in d), the locally-linear trend in c), and the time-varying process variance in e). In all figures, the posterior estimates for the time-varying effects are depicted with a red line, while the dotted blue lines stand for the 68% credible intervals for each posterior estimate. The time-varying proportion of variance in wine quality explained by temperature (R^2) is shown in f), for linear (green dotted line) and quadratic (blue dotted lines) effects, and their summed effects (thick red line). In g), the posterior estimates for the time-varying optimum growing season (GS) temperatures (^{0}C) are shown with a solid green line, while green and blue dotted lines represent 68% and 90% credible intervals for the estimates, respectively. For comparison, the observed temperature trend obtained with a smoothing LOESS function is shown as a yellow solid line. Note the logarithmic scale of the temperature axis.

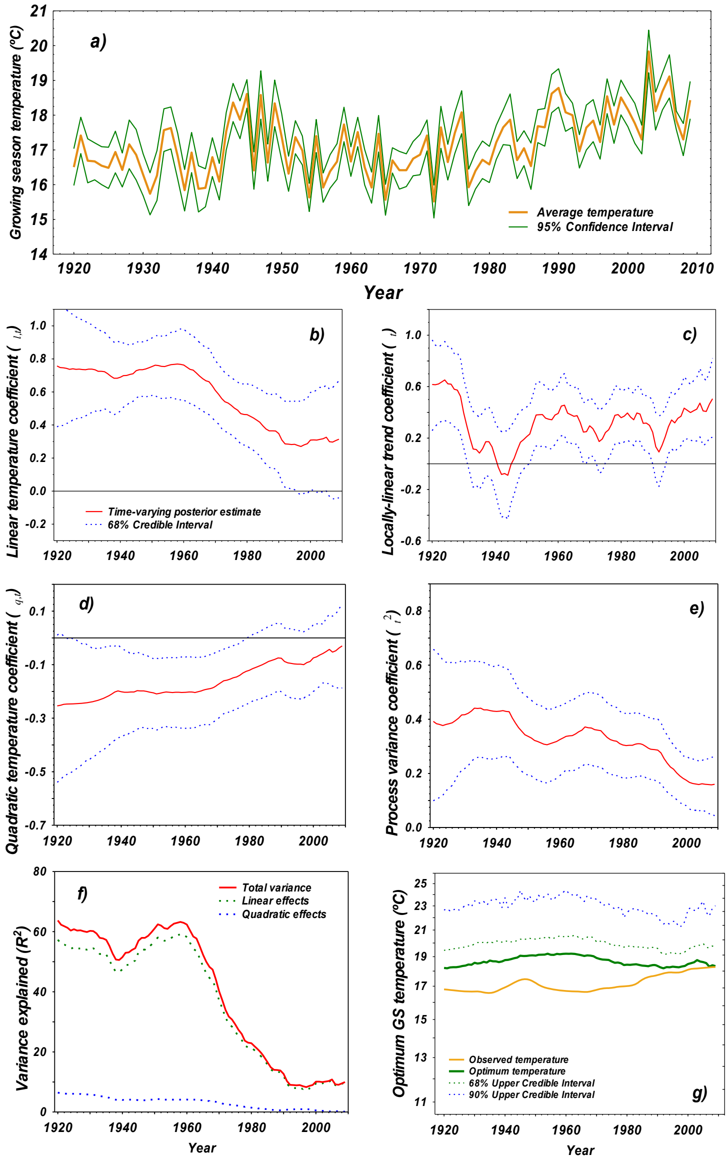

Figure S6: Comparison of several fits of the TVCs model to the time series of Tastet & Lawton wine quality ratings, assuming either no uncertainty in wine quality ratings (^{2} = 0) or increasing levels of uncertainty: from 1.5 x ^{2} (simulating a 50% increase in rating uncertainty) to 6 x ^{2}, equivalent to a 600% increase in rating uncertainty.

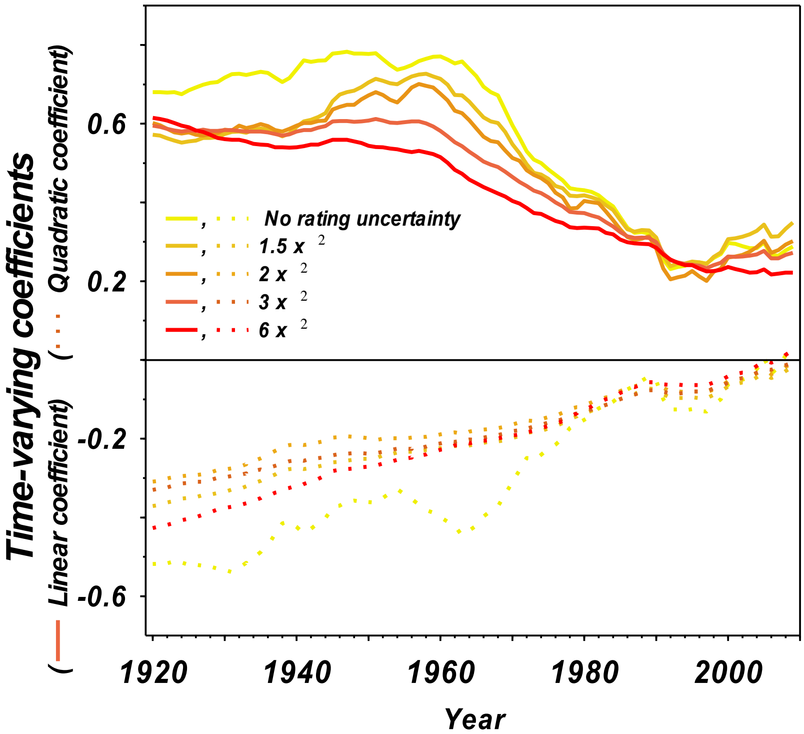

Figure S7: Results of the fitting of the TVCs model to the set of nonlinearly detrended time series of growing season temperatures (in a), standardized data) and wine quality ratings (in b), standardized data). The original data were regressed on year through a Generalized Additive Model using penalized likelihood estimation (Wood 2004); the model was selected using a penalized regression spline approach, with automatic smoothness selection through Generalized Cross-Validation. This method is highly efficient for removing complex (nonlinear) temporal trends. Figures in c) and d) show the linear and quadratic time-varying effects of temperature on wine quality, respectively, for the dataset in which only the growing season temperature data were detrended. Figures in e) and f) show the linear and quadratic time-varying effects of optimum growing season temperature on wine quality, respectively, for the dataset in which both the growing season temperature and wine quality rating time series were detrended.

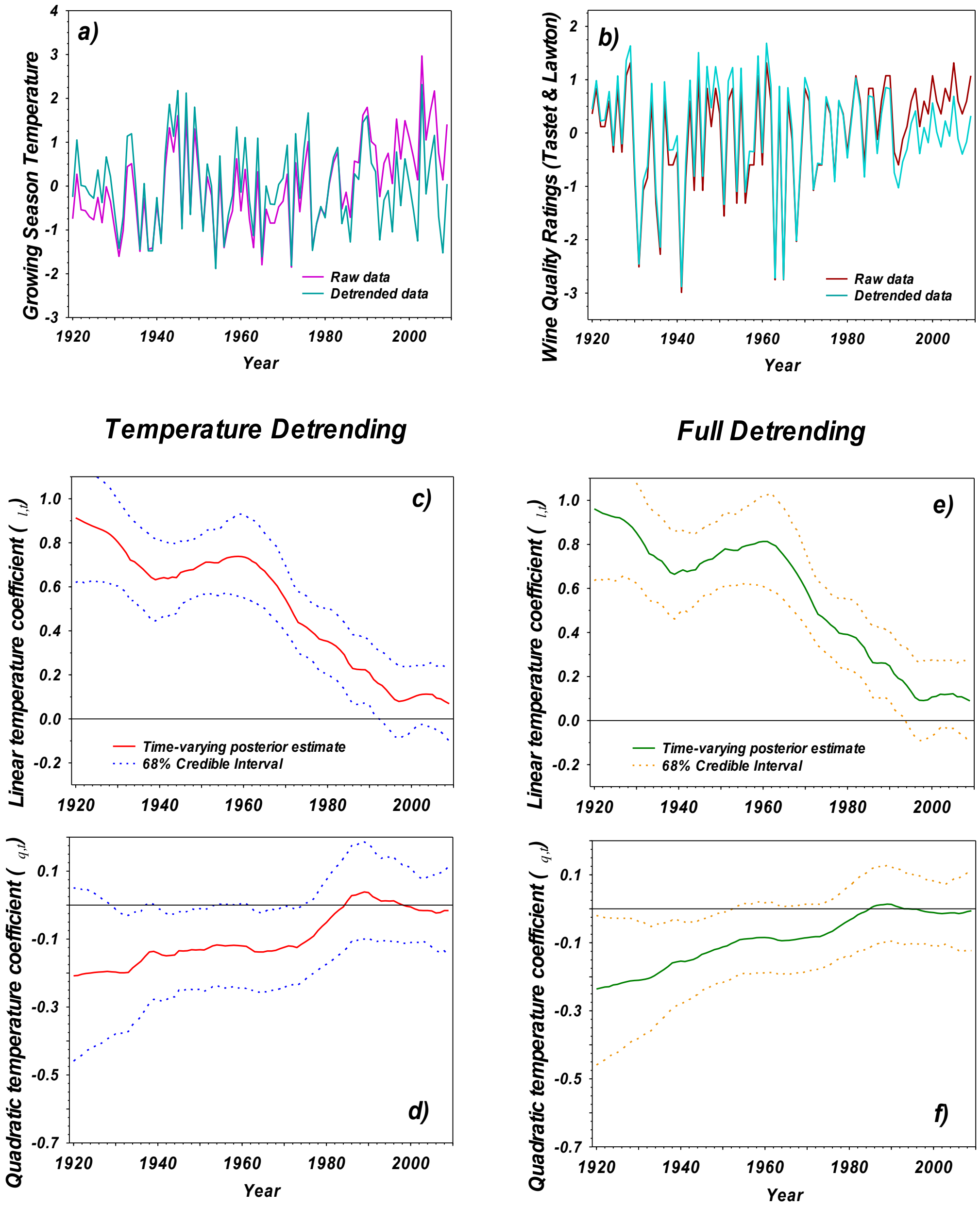

LITERATURE CITED

Arnfield AJ (2003) Two decades of urban climate research: a review of turbulence, exchanges of energy and water, and the urban heat island. International Journal of Climatology 23:1-26

Cardebat J-M, Figuet J-M (2013) Expert opinions and Bordeaux wine prices: an attempt to correct the bias of subjective judgments. AAWE Working Paper No. 129, ISSN 2166-9112

Carroll RJ, Ruppert D, Stefanski LA, Crainiceanu CM (2006) Measurement Error in Nonlinear Models: A Modern Perspective. Chapman and Hall/CRC, Boca Ratón, FL

Chevet JM, Lecocq S, Visser M (2011) Climate, grapevine phenology, wine production, and prices: Pauillac (1800-2009). American Economic Review 101:142-146

Clark JS (2007) Models for Ecological Data. Princeton University Press, Princeton NJ, USA

Duane S, Kennedy AD, Pendleton BJ, Roweth D (1987) Hybrid Monte Carlo. Physics Letters B 195:216–222.

Easterling DR, Peterson TC (1995) A new method for detecting undocumented discontinuities in climatological time series. International Journal of Climatology 15:369-377

Gelman A, Carlin JB, Stern HS, Dunson DB, Vehtari A, Rubin DB (2013a) Bayesian Data Analysis. Chapman &Hall/CRC Press, London, UK

Gelman A, Hwang J, Vehtari A (2013b) Understanding predictive information criteria for Bayesian models. Statistics and Computing 24: 997–1016

Grinsted A, Moore JC, Jevrejeva S (2004) Application of the cross wavelet transform and wavelet coherence to geophysical time series. Nonlin. Processes Geophys 11: 561–566

Hoffman MD, Gelman A (2013) The No-U-Turn sampler: adaptively setting path lengths in Hamiltonian Monte Carlo. Journal of Machine Learning Research 15:1351-1381

IPCC (2013) Climate Change 2013: The Physical Science Basis. Contribution of WGI to the Fifth assessment report of the IPCC. Cambridge University Press, Cambridge, UK

Jones GV, Davis RE (2000) Climate influences on grapevine phenology, grape composition, and wine production and quality for Bordeaux, France. Am. J. Viti. Enol. 51:249–261

Kalnay E, Cai M (2003) Impact of urbanization and land-use change on climate. Nature 423: 528–531

Lecocq S, Visser M (2006) Spatial variations in weather conditions and wine prices in Bordeaux. Journal of Wine Economics 1:114-124

Menne MJ, Williams Jr. CN (2009) Homogenization of temperature series via pairwise comparisons. Journal of Climate 22: 1700-1717

Neal R (2011) MCMC using Hamiltonian dynamics. In: Brooks S, Gelman A, Jones GL, Meng X-L (eds) Handbook of Markov Chain Monte Carlo. Chapman and Hall/CRC, p 116–162

Roberts P W, Reagans R (2007) Critical exposure and price-quality relationships for New World wines in the US market. Journal of Wine Economics 2:84-97

Stevenson T (2001) New Sotheby's Wine Encyclopedia: A Comprehensive Reference Guide to the Wines of the World, Dorling Kindersley, London, UK

West M, Harrison J (1997) Bayesian forecasting and dynamic models. Springer-Verlag, New York, USA

Wood SN (2004) Stable and efficient multiple smoothing parameter estimation for generalized additive models. J. Amer. Statist. Ass. 99:673-686